

Expression of connexin 43, ion channels and Ca²⁺-handling proteins in rat pulmonary vein cardiomyocytes

YAQIONG XIAO¹, XUE CAI², ANDREW ATKINSON², SUNIL JIT LOGANTHA²,
MARK BOYETT² and HALINA DOBRZYNSKI²

¹Department of Critical Care Medicine, Peking University International Hospital, Beijing 102206, P.R. China; ²Institute of Cardiovascular Sciences, Faculty of Medical and Human Sciences, University of Manchester, Manchester M13 9NT, UK

Received March 25, 2016; Accepted July 1, 2016

DOI: 10.3892/etm.2016.3766

Abstract. Atrial fibrillation (AF) is the most common cardiac arrhythmia. AF is thought to be triggered by ectopic beats, originating primarily in the myocardial sleeves surrounding the pulmonary veins (PVs). The mechanisms underlying these cardiac arrhythmias remain unclear. To investigate this, frozen sections of heart and lung tissue from adult rats without arrhythmia were obtained in different planes, stained with Masson's trichrome, and immunolabeled for connexin 43 (Cx43), caveolin-3 (Cav3), hyperpolarization-activated cyclic nucleotide-gated channel 4 (HCN4), Na_v1.5, Kir2.1, and the calcium handling proteins sarcoplasmic/endoplasmic reticulum calcium-ATPase 2a (SERCA2a) and ryanodine receptor 2 (RyR2). Transverse sections offered the best view of the majority of the PVs in the tissue samples. Cx43 was observed to be expressed throughout the atria, excluding the sinoatrial and atrioventricular nodes, and in the myocardial sleeves of the PVs. In contrast, HCN4 was only expressed in the sinoatrial and atrioventricular nodes. The immunodensity of Cav3, Na_v1.5, Kir2.1, SERCA2a and RyR2 in the PVs imaged was similar to that in atria. The results suggest that in the absence of arrhythmia, the investigated molecular properties of the ion channels of rat PV cardiomyocytes resemble those of the working myocardium. This indicates that ectopic beats originating in the myocardial sleeves of the PVs occur only under pathological conditions.

Introduction

Atrial fibrillation (AF) is the most common cardiac arrhythmia (1). AF has a prevalence of >2.3 million in the United States (2). Thromboembolism is the most serious complication

of AF, with a 5-fold increased risk of stroke (3). In addition, AF carries a 3-fold increased risk of heart failure (4,5), and a 2-fold increased risk of both dementia (6) and mortality (3,7).

Clinical AF can be categorized as paroxysmal, persistent or permanent (7). Paroxysmal AF, caused by focal drivers, particularly in the ectopic sites in myocardial sleeves around the pulmonary veins (PVs), can be eliminated by catheter ablation (8,9). The proximal tunica media of the PVs, typically referred to as the myocardial sleeve, is the primary source of supraventricular ectopic activity. This site includes the left atrial tissue extending to the PVs. However, the exact mechanisms by which AF occurs in the myocardial sleeve are not well-characterized, despite extensive studies (10-13).

Ectopic firing is driven by enhanced automaticity, early after depolarizations and delayed after depolarizations (DADs). The normal action potential in atrial cells remains at the resting potential following repolarization. The resting potential is maintained by high resting K⁺ permeability via inward rectifier K⁺ current (IK1). Pacemaker current (If) in atrial cells is overwhelmed by much larger IK1 with no manifestation of automaticity (14). Automaticity is attributed to decreased IK1 and/or enhanced If (1). DADs are caused by abnormal diastolic release Ca²⁺ from sarcoplasmic reticulum (SR) Ca²⁺ stores. Ryanodine receptor 2 (RyR2) is a specialized Ca²⁺ handling protein in the SR, which releases Ca²⁺ in response to transmembrane Ca²⁺ entry. Sarcoplasmic/endoplasmic reticulum Ca²⁺-ATPase 2a (SERCA2a) is another Ca²⁺ handling protein, which mediates the uptake of intracellular Ca²⁺ ([Ca²⁺]_i) in cardiomyocytes to maintain SR Ca²⁺ content. DADs are generated following [Ca²⁺]_i overload, for example in heart failure (15).

The conduction velocity of action potentials in the atria serves an important role in AF (1). Conduction velocity is primarily determined by inward currents causing depolarization (predominantly Na⁺) and gap junction channels (connexins) providing cell-to-cell electric continuity. In the PVs, conduction is also affected by myocardial sleeve disconnection and pattern, which may provide a substrate for re-entry in the veins (16-18).

In the present study, histological studies were performed to delineate the architecture of the PVs in rats. Furthermore, rat heart samples were immunolabeled for the following six possible markers of ectopic beat generation: Connexin 43 (Cx43), one of the most important gap junction channels; three ion channel proteins, the hyperpolarization-activated cyclic

Correspondence to: Dr Yaqiong Xiao, Department of Critical Care Medicine, Peking University International Hospital, 1 Life Park Road, Zhongguancun Life Science Park, Changping, Beijing 102206, P.R. China
E-mail: xiaoni2345@sina.com

Key words: atrial fibrillation, pulmonary vein, ectopic beat, ion channels, connexin 43

nucleotide-gated channel 4 (HCN4, responsible for I_f current); $\text{Na}_v1.5$ (mediates cardiac Na^+ current, I_{Na}); $\text{Kir}2.1$ (responsible for cardiac IK_1); and two Ca^{2+} handling proteins, SERCA2a and RyR2. All of the proteins being identified were considered to serve vital roles in ectopic beat generation, and thus may help elucidate the mechanisms of ectopic beat generation in the myocardial sleeves of PVs.

Materials and methods

Ethical approval. The experimental procedures in the present study were approved by the University of Manchester (Manchester, UK), and rats were handled in accordance with the United Kingdom Animals (Scientific Procedures) Act, 1986 (19). Rats were sacrificed in accordance with the current UK Home Office regulations on animal experimentation (20).

Animal and tissue preparation. In the present study 10 male adult Sprague-Dawley rats (3 months old; 200–450 g; Charles River UK, Ltd., Margate, UK) were used in the isolation of 7 hearts and 3 hearts + lungs. Rats were sacrificed by cervical dislocation, followed 15 min later by intraperitoneal injection of heparin (500 IU kg^{-1}). The heart + lungs were isolated by opening the thoracic cavity to expose the trachea. The exposed trachea was raised with fine forceps and a small V-shaped nicked on the top, followed by injection of between 3 and 4 ml Optimal Cutting Temperature (OCT) compound into the lungs and subsequent ligation of the trachea. The heart + lungs were then rapidly removed *en bloc* and washed in ice-cold phosphate buffered saline (PBS) solution. Hearts were isolated by separation from the lungs, the lungs were then dissociated from the hilum, leaving behind a fragment of lung tissue on the hearts, in order to retain the PVs, and washed with PBS. Samples were then embedded in OCT and frozen in isopentane (cooled in liquid nitrogen to -50°C). Coronal, transverse and sagittal sections of the heart were obtained. Transverse sections of connected heart and lung tissue were also obtained. Serial $20 \mu\text{m}$ cryosections at $100 \mu\text{m}$ intervals were collected from the samples onto Superfrost glass slides (Fisher Scientific; Thermo Fisher Scientific, Waltham, MA, USA) using a cryostat (Leica CM3050 S; Leica Biosystems, Nussloch, Germany) and stored at -80°C until required.

Histology. Bouin's fluid was used for 15 min to fix between 12 and 16 heart and heart + lung sections (at intervals of $400 \mu\text{m}$). Sections were then washed three times (10 min each) in 70% ethanol and stained with Masson's trichrome as previously described (21). Following staining, the tissue sections were dehydrated with a gradient of ethanol (70 to 100%), cleared in Histo-Clear (National Diagnostics, Hesse, UK) and mounted with DPX mounting medium (Merck KGaA, Darmstadt, Germany). Using this technique, nuclei were stained dark blue/black, cardiomyocytes were stained purple and connective tissue blue. Stained samples were stored at room temperature prior to analysis by light microscopy.

Antibodies. Eight primary antibodies were used in this study: Mouse anti-Cx43 (polyclonal; 1:200; cat. no. AB1727; Chemicon, Livingston, UK); rabbit anti-Cx43 (polyclonal; 1:200; cat. no. C6219; Sigma-Aldrich, St. Louis, MO, USA); rabbit anti-HCN4 (polyclonal; 1:50; cat. no. APC-052; Alomone Labs,

Jerusalem, Israel); mouse anti-caveolin-3 (Cav3) (monoclonal; 1:500; cat. no. 610420; BD Biosciences, Oxford, UK); mouse anti-RyR2 (clone C3-33; monoclonal; 1:100; cat. no. MA3-916; Thermo Fisher Scientific); mouse anti-SERCA1/2 (clone Y/1F4; monoclonal; 1:100; cat. no. A010-21AP; Badrilla, Ltd., Leeds, UK); rabbit anti- $\text{Na}_v1.5$, corresponding to amino acid residues 493–511 (polyclonal; 1:50; cat. no. ASC-005; Alomone Labs); and rabbit anti- $\text{Kir}2.1$, corresponding to amino acid residues 392–410 (polyclonal; 1:50; cat. no. APC-026; Alomone Labs). The secondary antibodies used were the following: Donkey anti-mouse conjugated to cyanine 3 (Cy3) polyclonal antibody (1:500; cat. no. AP192C; Chemicon, Rolling Meadows, Illinois, USA); donkey anti-rabbit conjugated to Cy3 polyclonal antibody (1:500; cat. no. AP182C; Chemicon, Rolling Meadows, Illinois, USA); and donkey anti-rabbit conjugated to fluorescein isothiocyanate (FITC) (polyclonal; 1:100; cat. no. sc-2090; Santa Cruz Biotechnology, Inc., Dallas, Texas, USA).

Immunohistochemistry. Immunohistochemistry was conducted using sections adjacent to those used for histology. Briefly, sections were fixed with 10% buffered formalin (Sigma-Aldrich) for 30 min and then washed with 0.01 M PBS (Sigma-Aldrich) three times at 10 min intervals. Sections were then treated with 0.1% Triton X-100 in PBS for 30 min, washed with PBS and blocked in 1% bovine serum albumin (BSA; Sigma-Aldrich) in PBS for 1 h at room temperature. Sections were incubated with the appropriate primary antibody (diluted in 1% BSA in PBS) at 4°C overnight, washed three times with PBS over 30 min and then incubated with the appropriate secondary antibodies for between 90 and 120 min at room temperature in the dark. Following three washes in PBS, coverslips were applied to the slides using VECTASHIELD Mounting Medium (cat. no. H-1000; Vector Laboratories, Inc., Burlingame, CA, USA) and sealed with a nail varnish. Slides were stored in the dark at 4°C prior to analysis by confocal microscopy.

Confocal microscopy. Images representing single optical sections were acquired using a confocal laser scanning microscope (LSM 510; Zeiss, Oberkochen, Germany) equipped with argon and helium-neon lasers, at excitation wavelengths of 488 and 568 nm to detect FITC and Cy3 respectively.

Results

Morphology of rat PVs. Heart and heart + lung samples stained with Masson's trichrome were used for histology of the PVs. Transverse tissue sections of heart samples were stained purple for cardiomyocytes of the heart and PVs, blue for connective tissue and navy/black for nuclei (Figs. 1 and 2). The transverse view of the PVs allowed for the visualization of portions of the four PVs and left superior vena cava. The PVs extending from the atria narrowed as they terminated in the lungs. However, the myocardial sleeves of the PVs varied in thickness. For example, cardiomyocytes in the right superior PV (RSPV) formed triangular regions that extended into the loose adventitia (Fig. 1A, indicated by the thick red arrow). The walls of the PVs comprised three layers as follows: A thin compact layer close to the lumen of the intima, a middle layer of cardiomyocytes and an outer layer of loose adventitia (Figs. 1D and 2D).

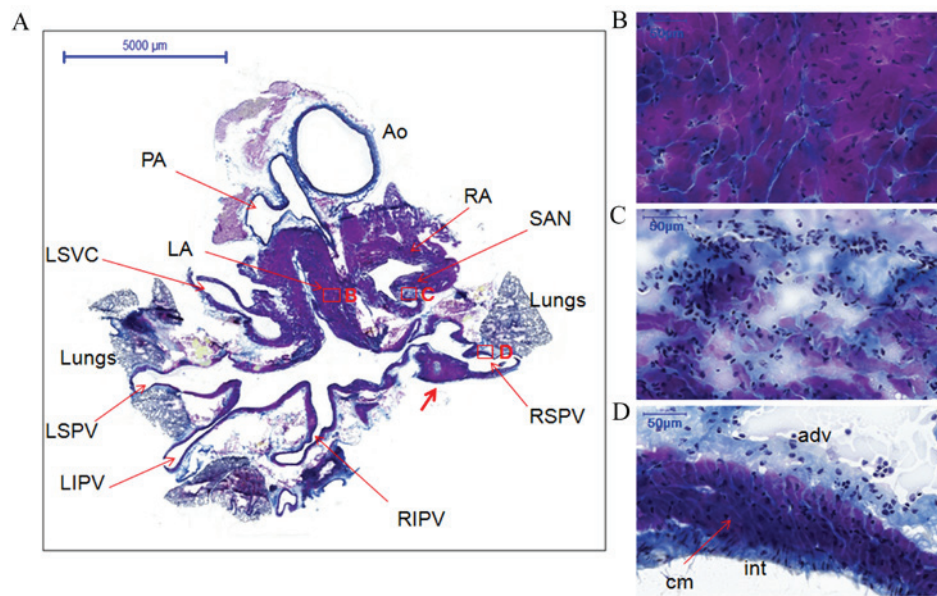


Figure 1. Histology of the pulmonary veins from transverse sections of the whole heart of rats without arrhythmia stained with Masson's trichrome. (A) Whole heart section showing the locations of different structures, boxes represent the locations of B, C and D (scale bar, 5,000 μ m). The thick red arrow indicates cardiomyocytes in the RSPV that formed triangular regions that extended into the loose adventitia. (B) LA (scale bar, 50 μ m). (C) SAN (scale bar, 50 μ m). (D) RSPV (scale bar, 50 μ m). Cardiomyocytes of the heart and PVs are stained purple, connective tissue blue and nuclei navy/black. AO, aorta; PA, pulmonary artery; RA, right atrium; LA, left atrium; SAN, sinoatrial node; RSPV, right superior pulmonary vein; RIPV, right inferior pulmonary vein; RSPV, left superior pulmonary vein; LIPV, left inferior pulmonary vein; LSVC, left superior vena cava; int, intima; cm, cardiomyocytes; adv, adventitia.

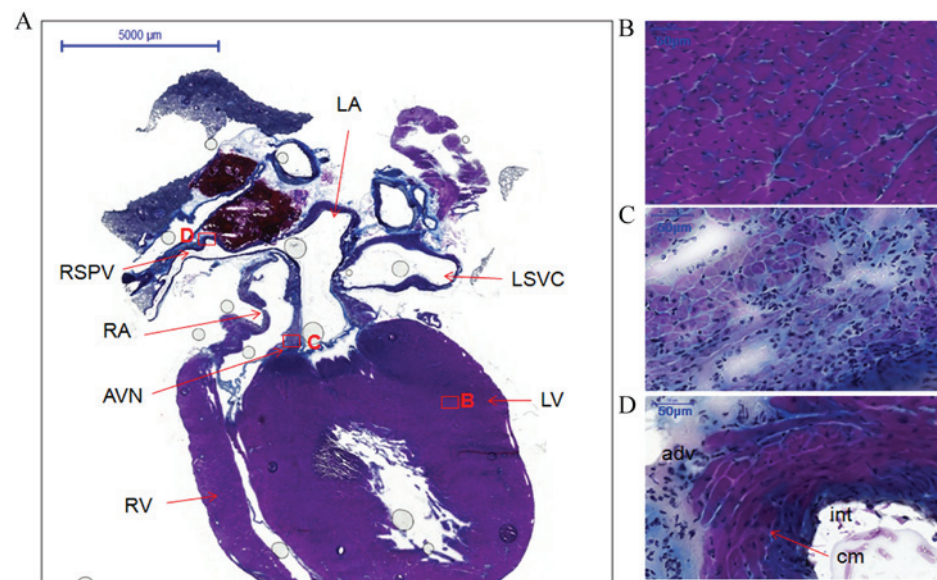


Figure 2. Histology of the atria, ventricles, atrioventricular node and right superior pulmonary vein from coronal sections of the whole heart of rats without arrhythmia stained with Masson's trichrome. (A) Coronal view of whole heart section showing locations of different structures, boxes represent the locations of B, C and D (scale bar, 5,000 μ m). (B) LV (scale bar, 50 μ m). (C) AVN (scale bar, 50 μ m). (D) RSPV (scale bar, 50 μ m). LA, left atrium; RA, right atrium; LV, left ventricle; RV, right ventricle; AVN, atrioventricular node; RSPV, right superior pulmonary vein; LSVC, left superior vena cava; int, intima; cm, cardiomyocytes; adv, adventitia.

The coronal section from another heart specimen showed the two atria, two ventricles, the atrioventricular node and one right PV (Fig. 2A). The working myocardium [left ventricle (LV)] and PV cardiomyocytes were heavily stained (Fig. 2B and D, respectively). However, the cardiomyocytes in the atrioventricular node and the sinoatrial node were lightly stained (Figs. 2C and 1C). Furthermore, the cellular orientation in the sinoatrial node (Fig. 1C) was disorganized compared with the working myocardium (LA; Fig. 1B) and PVs (RSPV; Fig. 1D).

PVs express Cx43 but not HCN4. PV expression of Cx43 and HCN4 was investigated (Figs. 3 and 4). HCN4 protein was detected (green signal) in the plasma membrane of the sinoatrial node (green signal; Fig. 3A) and the atrioventricular node (data not shown). However, only a very weak HCN4 signal was detected in the working myocardium [green signal; left atrium (LA); Fig. 3B] and throughout the myocardial sleeves (Fig. 3C and D). Cx43 was identified in the working myocardium (red signal; LA; Fig. 3B and green signal; LA;

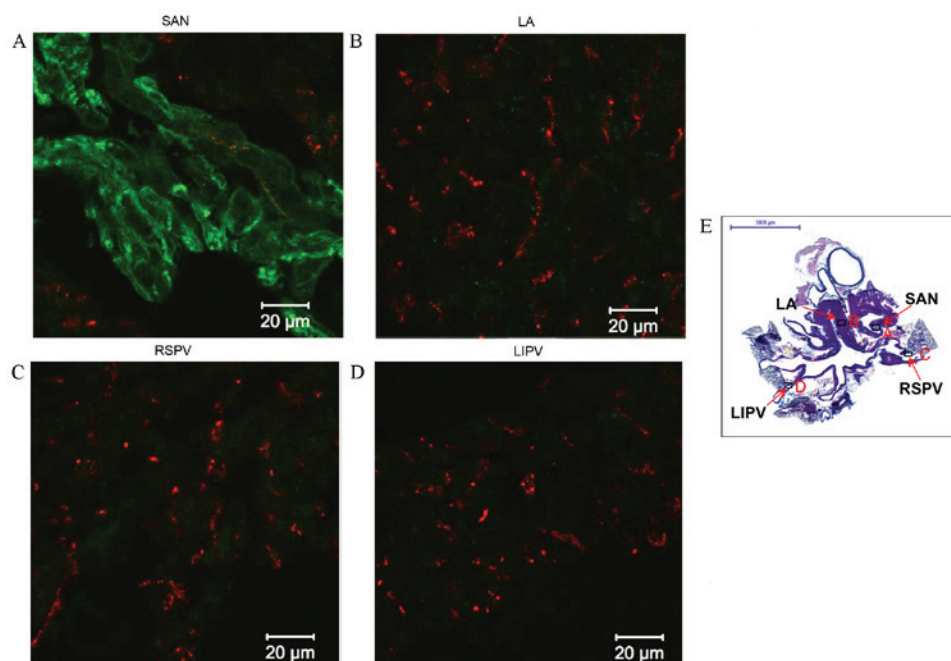


Figure 3. Immunohistochemistry of hyperpolarization-activated cyclic nucleotide-gated channel 4 (HCN4) and connexin 43 (Cx43) expression in transverse sections of the whole heart of rats without arrhythmia. Expression of HCN4 (green) and Cx43 (red) in the (A) SAN, (B) LA, (C) RSPV and (D) LIPV. Scale bar, 20 μm. (E) Masson's trichrome-stained transverse section of the whole heart, boxes represent the locations of A, B, C and D. Scale bar, 5,000 μm. LA, left atrium; SAN, sinoatrial node; RSPV, right superior pulmonary vein; LIPV, left inferior pulmonary vein.

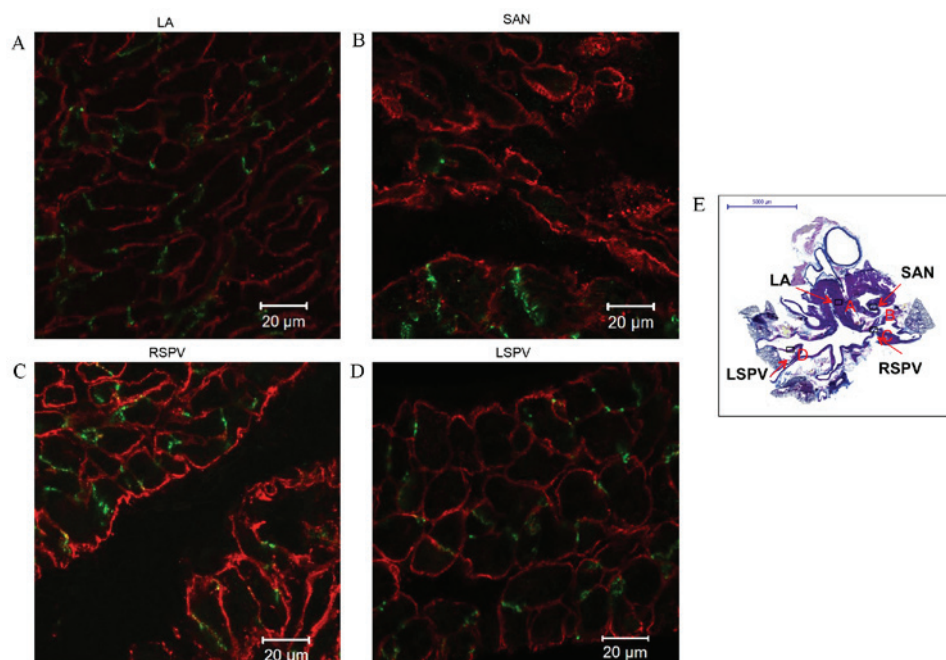


Figure 4. Immunohistochemistry of connexin 43 (Cx43) and caveolin 3 (Cav3) expression in transverse sections of the whole heart of rats without arrhythmia. Expression of Cx43 (green) and Cav3 (red) in the (A) LA, (B) SAN, (C) RSPV and (D) LSPV. Scale bar, 20 μm. (E) Masson's trichrome-stained transverse section of the whole heart, boxes represent the locations of A, B, C and D. Scale bar, 5,000 μm. LA, left atrium; SAN, sinoatrial node; RSPV, right superior pulmonary vein; LSPV, left superior pulmonary vein.

Fig. 4A), the PVs (red signal; Fig. 3C and D and green signal in Fig. 4C and D), but had a very weak signal in the sinoatrial node (Figs. 3B and 4B, red and green signals, respectively). The cardiac biomarker Cav3 was detected in cardiomyocytes of the working myocardium (red signal; LA; Fig. 4A), the cardiac conduction system, such as the sinoatrial node (red

signal; Fig. 4B), and the PVs (red signal; Fig. 4C and D). Cav3 expression in the PVs (stained purple in Figs. 1D and 2D) confirms the presence of cardiomyocytes in PVs.

Shared protein expression patterns between the myocardial sleeves of PVs and the working myocardium. Protein expression

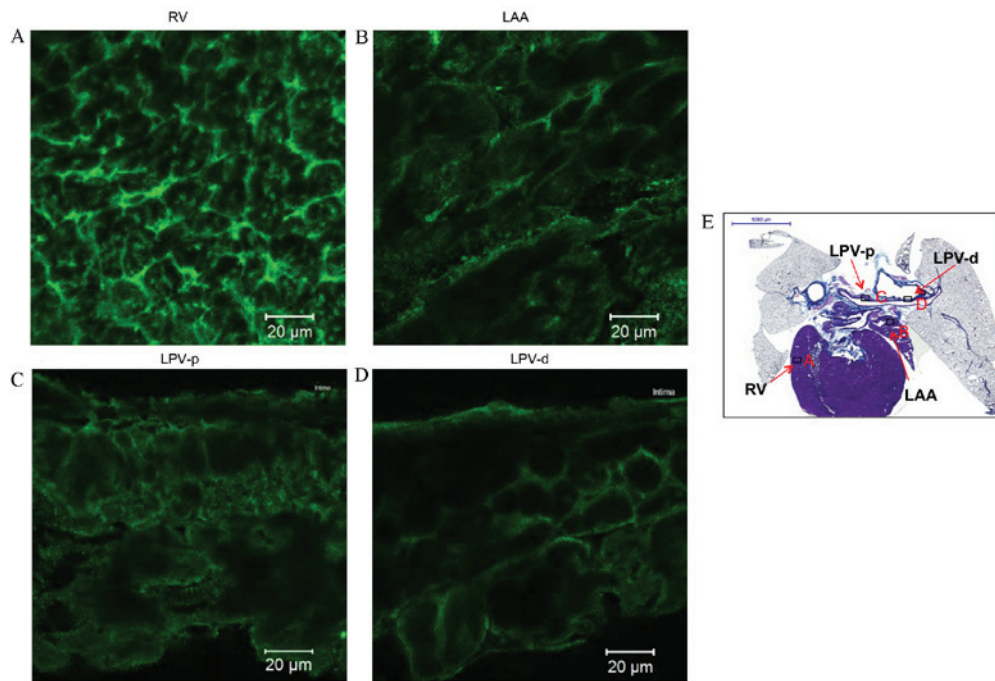


Figure 5. Immunohistochemistry of $\text{Na}_v1.5$ expression in transverse heart + lung sections of rats without arrhythmia. Expression of $\text{Na}_v1.5$ in the (A) RV, (B) LAA, (C) LPV-p and (D) LPV-d. Scale bar, 20 μm . (E) Masson's trichrome-stained transverse section of the whole heart, boxes represent the locations of A, B, C and D. Scale bar, 5,000 μm . RV; right ventricle; LAA, left arterial appendage; LPV-p, proximal left pulmonary vein; LPV-d, distal pulmonary vein.

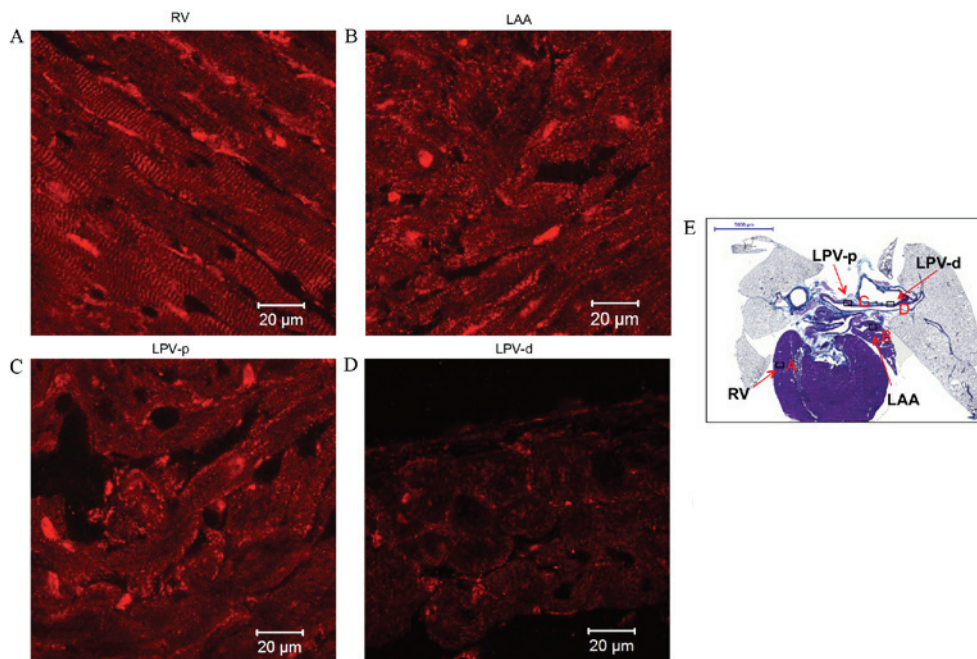


Figure 6. Immunohistochemistry of $\text{Kir}2.1$ expression in transverse heart + lung sections of rats without arrhythmia. Expression of $\text{Kir}2.1$ in the (A) RV, (B) LAA, (C) LPV-p and (D) LPV-d. Scale bar, 20 μm . (E) Masson's trichrome-stained transverse section of the whole heart, boxes represent the locations of A, B, C and D. Scale bar, 5,000 μm . RV; right ventricle; LAA, left arterial appendage; LPV-p, proximal left pulmonary vein; LPV-d, distal pulmonary vein.

patterns of the myocardial sleeves of PVs and the working myocardium were investigated to identify any similarities (Figs. 5-8). The present study detected that $\text{Na}_v1.5$ expression (green signal) in the working myocardium, including the right ventricle (RV) and left atrial appendage (LAA) (Fig. 5A and B, respectively). $\text{Na}_v1.5$ was also expressed in PV tissue, such as the left PV (LPV; Fig. 5C and D). Expression of $\text{Na}_v1.5$ was higher in

the RV (Fig. 5A) compared with the other tissues investigated. $\text{Kir}2.1$ expression (red signal) was similar to that of $\text{Na}_v1.5$, and was detected in the working myocardium (such as the RV and LAA in Fig. 6A and B respectively) and PVs (such as LPV shown in Fig. 6C and D). $\text{Kir}2.1$ was more highly expressed in the RV (Fig. 6A) compared with the other tissues investigated. The striated pattern of $\text{Kir}2.1$ expression observed in Fig. 6A

Table I. Proteins expressed in the working myocardium, sinoatrial node and pulmonary veins.

| Protein | PVs | LA | LV | RV | RA | SAN |
|---------------------|-----|----|----|----|----|-----|
| Cav3 | + | + | + | + | + | + |
| Cx43 | + | + | + | + | + | - |
| HCN4 | - | - | - | - | - | + |
| Na _v 1.5 | ± | ± | + | + | ± | N/A |
| Kir2.1 | ± | ± | + | + | ± | N/A |
| RyR2 | + | + | + | + | + | N/A |
| SERCA2a | + | + | + | + | + | N/A |

Symbols in the table indicate the following: +, presence; -, absence; and ±, weak presence of the indicated protein. N/A, no data collected. PVs, pulmonary veins; LA, left atrium; LV, left ventricle; RV, right ventricle; RA, right atrium; SAN, sinoatrial node; Cav3, caveolin-3; Cx43, connexin 43; HCN4, hyperpolarization-activated cyclic nucleotide-gated channel 4; RyR2, ryanodine receptor 2; SERCA2a, sarcoplasmic/endoplasmic reticulum calcium-ATPase 2a; N/A, not applicable.

likely corresponds to t-tubules. The Kir2.1 signal intensity in the PVs (Fig. 6C and D) was comparable with that in the LAA (Fig. 6B), but was weaker compared with the RV (Fig. 6A).

RyR2 (red signal) was abundantly expressed in a striated pattern intracellularly in the working myocardium, particularly in the area close to the cell surface (Fig. 7A and C), and in the LPV (Fig. 7D). Two layers of myofibers were oriented differently in the LPV: One layer circumferentially around the lumen and the other longitudinal to the LPV (Fig. 7D). In addition, an intense and uniform reticular pattern of SERCA2a expression was identified in the working myocardium, including the RV, right atrium (RA) and LA (Fig. 8A-C, respectively). SERCA2a expression in the RSPV (Fig. 8D) was similar to that of the working myocardium. A summary of the proteins expressed in the working myocardium, sinoatrial node and PVs is shown in Table I.

Discussion

In the present study the histology and immunohistochemistry of the PVs in adult rats without arrhythmia was investigated. It was observed that the myocardial sleeves of the PVs extended from the atria into the lungs. PV cardiomyocytes were determined to express Cx43, Cav3, Na_v1.5, Kir2.1, RyR2 and SERCA2a, but not HCN4, at levels similar to the LA.

In 2008, a study reported the differences in the histology of PVs between rodents and humans (22). Mice and rat cardiomyocytes were found to typically extend along the PVs from the hilus into the lung. However human extrapericardiac cardiomyocytes were found in <30% of PVs and exhibited an incomplete sleeve at the hilus. Furthermore, in humans, cardiomyocytes were determined to occur significantly more often in the RPVs than the LPVs and never in PVs within the lungs. The present study identified the presence of rat cardiomyocytes in PVs within the lungs, through staining of the cardiomyocytes and identifying expression Cav3, which is concentrated in the caveolae of cardiomyocytes.

Consistent with the present study's identification of the presence of rat cardiomyocytes in PVs within the lung, a previous study demonstrated the occurrence of electrically-induced action potentials in rat cardiomyocytes of the distal PV in all lobes of the lung (23). The action potentials were triangular and atrial (23). In addition, prior research showed that the shape of PV action potentials was similar to that recorded in the left atrial cells of dogs and humans (17,24). However, another study reported that, compared with the left atrial free-wall, canine PV cardiomyocytes were characterized by lower negative resting membrane potentials, a lower maximum phase 0 upstroke velocity and shorter action potential duration (25).

Gap junction channels consisting of connexins mediate the electric coupling between cardiomyocytes. Electric coupling in the working myocardium is strong, allowing rapid conduction of action potentials. However, poor electric coupling within the sinoatrial node results in slow conduction (26,27), which protects the pacemaking tissue from the hyperpolarizing effect of the surrounding atrial muscle (28). Gap junctions are clustered channels consisting of two hemichannels, each formed by 6 Cx proteins, which connect the cytoplasm of adjacent cardiomyocytes (29). Three principal connexins are expressed in cardiomyocytes, Cx43, Cx40, and Cx45 (30). Cx43 is expressed in all chambers of the heart. In the present study, Cx43 expression in the PVs was similar to that in the working myocardium, but in contrast to that in the cardiac conduction system (such as the sinoatrial node). This finding indicates that the electric coupling between PV cardiomyocytes is similar to that in the working myocardium. Previous studies have found that presence of AF was accompanied with a reduction in atrial Cx43, and that Cx43 gene therapy prevents persistent AF in animal models (31,32), indicating that Cx43 serves a critical role in AF. Therefore, the abundant PV expression of Cx43 found in the present study strongly suggests that PV cardiomyocytes are electrically well coupled, in contrast with the sinoatrial node.

The present study investigated three key cardiac ion channels; HCN4, Na_v1.5 and Kir2.1. Firstly, HCN4 protein was identified to be present in the sinoatrial node, but only in very small quantities in the atria and PVs. HCN4 is the primary HCN isoform, responsible for the pacemaker current (If). HCN4 is highly expressed in the sinoatrial nodes, but not PVs, of small mammals and humans (33). However, one study reported that sinoatrial node-like tissue is present in human PVs containing the principal cells of the sinus node (P cells), transitional cells and Purkinje cells (34). In addition, HCN4 expression in interstitial Cajal cells is capable of generating a repetitive electrical rhythm within human PVs, particularly in patients with a history of AF (35). The present study determined that there were no ectopic focus cells that expressed HCN4 in the PVs of adult rats without arrhythmia. Interestingly, a recent study found that expression levels of HCN2 and HCN4 channel mRNA and protein were lower in the sinoatrial node, and higher in the atrium and PVs of aged dogs, suggesting that atrial electrophysiology and regional HCN2 and HCN4 channel expression are associated with the onset and maintenance of age-related AF (36).

Secondly, the present study identified that Na_v1.5, responsible for cardiac INa, is present in the PVs and the working myocardium of rats without AF. Expression of Na_v1.5 in the PVs, although weaker than that in the ventricles, was similar to

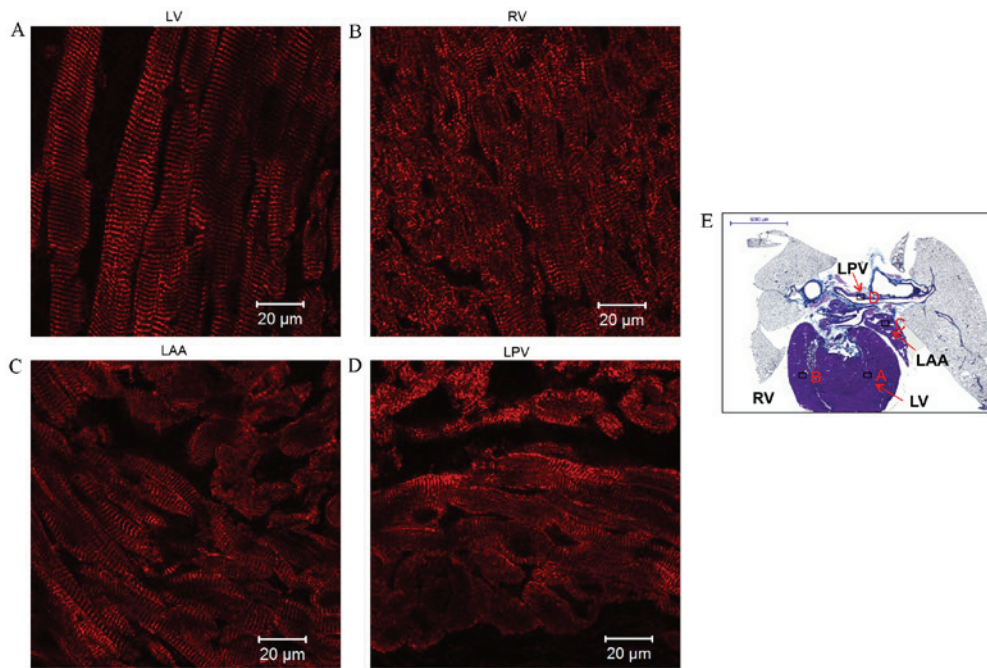


Figure 7. Immunohistochemistry of ryanodine receptor 2 (RyR2) expression in transverse sections of the heart + lungs of rats without arrhythmia. Expression of RyR2 in the (A) LV, (B) RV, (C) LAA and (D) LPV. Scale bar, 20 μ m. (E) Masson's trichrome-stained transverse section of the whole heart, boxes represent the locations of A, B, C and D. Scale bar, 5,000 μ m. LV, left ventricle; RV, right ventricle; LAA, left atrial appendage; LPV, left pulmonary vein.

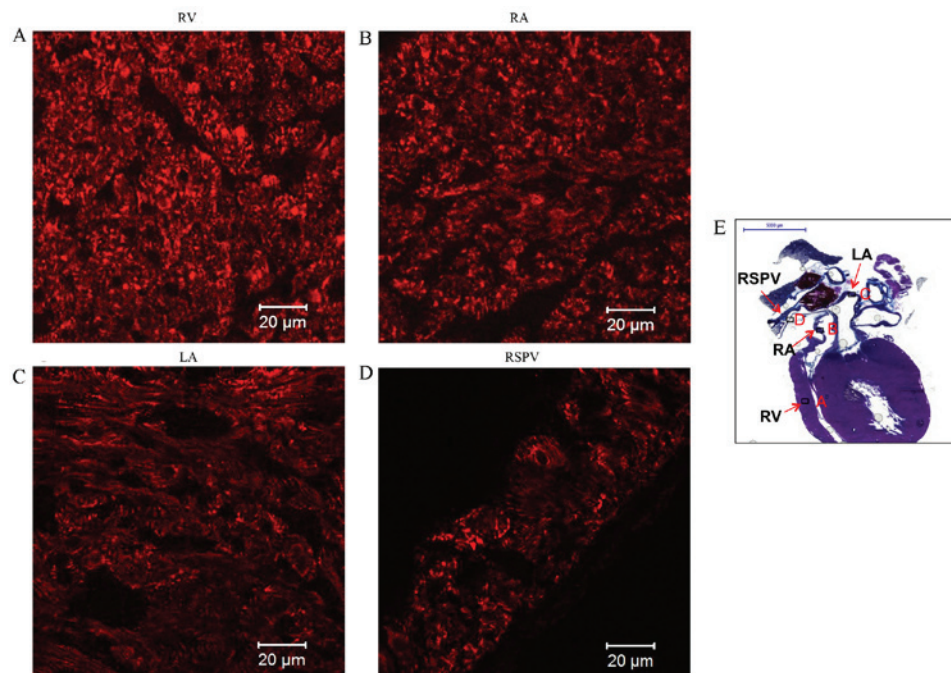


Figure 8. Immunolabeling of sarcoplasmic/endoplasmic reticulum calcium-ATPase 2a (SERCA2a) expression in coronal sections of the whole heart of rats without arrhythmia. Expression of SERCA2a in the (A) RV, (B) RA, (C) LA and (D) RSPV. Scale bar, 20 μ m. (E) Masson's trichrome-stained coronal section of the whole heart, boxes represent the locations of A, B, C and D, scale bar, 5,000 μ m. RV, right ventricle; RA, right atrium; LA, left atrium; RSPV, right superior pulmonary vein.

that in the atria. In contrast, a previous study found that $\text{Na}_v1.5$ was absent in the majority of sinoatrial node cells (28). This suggests that there is differential expression of $\text{Na}_v1.5$ in PVs and the sinoatrial node.

Thirdly, the results of the present study determined that the Kir2.1 expression profile in the PVs is similar to that of $\text{Na}_v1.5$.

Kir2.1 expression is associated with IK1. In the working myocardium, IK1 serves an important role in the final phase repolarization of the action potential and in the generation of resting membrane potential (37). Weak Kir2.1 expression in the sinoatrial node compared with the atrial muscle leads to a lack of stable resting potential in the sinoatrial node (21,28).

Chen *et al* (38) reported that canine PV cardiomyocytes with spontaneous activity have a significantly lower IK1 density. However, the present study found that the Kir2.1 expression in the PVs was similar to that in the atrium. This result suggests that unlike the sinoatrial node cells, cardiomyocytes of the PVs have a more stable resting potential. Although, a previous study suggested that lower levels and the subcellular distribution of Kir2.3 in canine PVs may contribute to their smaller IK1 density (39).

Finally, the present study investigated two Ca^{2+} -handling proteins, RyR2 and SERCA2a. In the heart, $[\text{Ca}^{2+}]_i$ movements regulate subsequent mechanical contractions. In cardiac excitation-contraction coupling, RyR2 represents the SER Ca^{2+} release channel. SERCA2a is a Ca^{2+} -ATPase that transfers Ca^{2+} from the cytosol of cardiomyocytes to the lumen of the SR, at the expense of ATP hydrolysis. During systole, Ca^{2+} is released from the SR through the RyR2. Subsequently, Ca^{2+} binds to troponin C and initiates the cross-bridge movement of the myofibrils, resulting in force development and contraction. During diastole, SERCA2a rapidly sequesters Ca^{2+} into the SR for cardiac relaxation (40,41). The present study compared the expression of RyR2 and SERCA2a between PVs and working myocytes. RyR2 and SERCA2a were identified in the PVs and the working myocytes, as previously reported (42,43). Their pattern of expression in PV cardiomyocytes resembled the pattern found in the atria, which explains the molecular basis of their contractile response to electrical excitation (44,45). In addition, intracellular Ca^{2+} serves an important role in pacemaking in small mammals (46). RyR2 dysregulation and enhanced SERCA2a activity increase SR Ca^{2+} leakage and release events, causing DADs in paroxysmal AF. Although the expression of the Na^+ - Ca^{2+} exchanger does not vary between tissues, RyR2 and SERCA2a were identified to be less abundant in the sinoatrial node than in atrial cells in humans (21). In the present study, similar expression patterns of RyR2 and SERCA2a were found between PV cardiomyocytes and atrial cells in adult rats without arrhythmia. This indicates different expression patterns of RyR2 and SERCA2a between PV cardiomyocytes and the sinoatrial node. PV arrhythmogenesis, caused by abnormal Ca^{2+} regulation likely occurs only under pathological conditions, such as heart failure and dilated atria, resulting in remodeling of Ca^{2+} -handling proteins and altered intracellular Ca^{2+} dynamics (47).

The present study had a number of limitations. Firstly, data was derived from adult rats without arrhythmia, which does not address the clinical realities of AF. Electrical remodeling in the myocardial sleeves of the PVs under pathological conditions may contribute to ectopic beats. Secondly, only histological and immunohistochemical studies were conducted. Minor differences between cardiomyocytes of rat PVs vs. left atrium were undetectable due to methodological constraints. Therefore, further investigations are needed to elucidate the molecular mechanisms contributing to the generation of ectopic beats.

In conclusion, the expression of Cx43, the three key cardiac ion channels (HCN4, Nav1.5 and Kir2.1) and the two Ca^{2+} -handling proteins (RyR₂ and SERCA2a) in the PVs of adult rats without arrhythmia is similar to that in the working

myocardium, but unlike the sinoatrial node. The results of the present study suggested that PV cardiomyocytes of adult rats without arrhythmia are electrically well coupled and have a stable resting potential. This indicates that ectopic beats originating in the myocardial sleeves surrounding the PVs are likely associated with pathological conditions, such as heart failure.

Acknowledgements

The authors would like to thank Mr Joseph Yanni Gerges from the Institute of Cardiovascular Sciences, Faculty of Medical and Human Sciences, University of Manchester, UK for assistance with immunohistochemical staining.

References

1. Iwasaki YK, Nishida K, Kato T and Nattel S: Atrial fibrillation pathophysiology: Implications for management. *Circulation* 124: 2264-2274, 2011.
2. Chen LY and Shen WK: Epidemiology of atrial fibrillation: A current perspective. *Heart Rhythm* 4 (3 Suppl): S1-S6, 2007.
3. Kannel WB, Wolf PA, Benjamin EJ and Levy D: Prevalence, incidence, prognosis, and predisposing conditions for atrial fibrillation: Population-based estimates. *Am J Cardiol* 82: 2N-9N, 1998.
4. Wang TJ, Larson MG, Levy D, Vasan RS, Leip EP, Wolf PA, D'Agostino RB, Murabito JM, Kannel WB, Benjamin EJ: Temporal relations of atrial fibrillation and congestive heart failure and their joint influence on mortality: The framingham heart study. *Circulation* 107: 2920-2925, 2003.
5. Stewart S, Hart CL, Hole DJ and McMurray JJ: A population-based study of the long-term risks associated with atrial fibrillation: 20-year follow-up of the Renfrew/Paisley study. *Am J Med* 113: 359-364, 2002.
6. Ott A, Breteler MM, de Bruyne MC, van Harskamp F, Grobbee DE and Hofman A: Atrial fibrillation and dementia in a population-based study. The rotterdam study. *Stroke* 28: 316-321, 1997.
7. January CT, Wann LS, Alpert JS, Calkins H, Cigarroa JE, Cleveland JC Jr, Conti JB, Ellinor PT, Ezekowitz MD, Field ME, *et al*: 2014 AHA/ACC/HRS guideline for the management of patients with atrial fibrillation: A report of the American College of Cardiology/American Heart Association Task Force on Practice Guidelines and the Heart Rhythm Society. *J Am Coll Cardiol* 64: e1-e76, 2014.
8. Haissaguerre M, Jaïs P, Shah DC, Takahashi A, Hocini M, Quiniou G, Garrigue S, Le Mouroux A, Le Métayer P and Clémenty J: Spontaneous initiation of atrial fibrillation by ectopic beats originating in the pulmonary veins. *N Engl J Med* 339: 659-666, 1998.
9. Cappato R, Calkins H, Chen SA, Davies W, Iesaka Y, Kalman J, Kim YH, Klein G, Natale A, Packer D, *et al*: Updated worldwide survey on the methods, efficacy, and safety of catheter ablation for human atrial fibrillation. *Circ Arrhythm Electrophysiol* 3: 32-38, 2010.
10. Po SS, Li Y, Tang D, Liu H, Geng N, Jackman WM, Scherlag B, Lazzara R and Patterson E: Rapid and stable re-entry within the pulmonary vein as a mechanism initiating paroxysmal atrial fibrillation. *J Am Coll Cardiol* 45: 1871-1877, 2005.
11. Corradi D, Callegari S, Gelsomino S, Lorusso R and Macchi E: Morphology and pathophysiology of target anatomical sites for ablation procedures in patients with atrial fibrillation: Part II: Pulmonary veins, caval veins, ganglionated plexi, and ligament of Marshall. *Int J Cardiol* 168: 1769-1778, 2013.
12. Tan AY, Li H, Wachsmann-Hogiu S, Chen LS, Chen PS and Fishbein MC: Autonomic innervation and segmental muscular disconnections at the human pulmonary vein-atrial junction: Implications for catheter ablation of atrial-pulmonary vein junction. *J Am Coll Cardiol* 48: 132-143, 2006.
13. Nathan H and Gloobe H: Myocardial atrio-venous junctions and extensions (sleeves) over the pulmonary and caval veins. Anatomical observations in various mammals. *Thorax* 25: 317-324, 1970.

14. Stillitano F, Lonardo G, Zicha S, Varro A, Cerbai E, Mugelli A and Nattel S: Molecular basis of funny current (If) in normal and failing human heart. *J Mol Cell Cardiol* 45: 289-299, 2008.
15. Yeh YH, Wakili R, Qi XY, Chartier D, Boknik P, Käb S, Ravens U, Coutu P, Dobrev D and Nattel S: Calcium-handling abnormalities underlying atrial arrhythmogenesis and contractile dysfunction in dogs with congestive heart failure. *Circ Arrhythm Electrophysiol* 1: 93-102, 2008.
16. Hocini M, Ho SY, Kawara T, Linnenbank AC, Potse M, Shah D, Jais P, Janse MJ, Haïssaguerre M and De Bakker JM: Electrical conduction in canine pulmonary veins: Electrophysiological and anatomic correlation. *Circulation* 105: 2442-2448, 2002.
17. Verheule S, Wilson EE, Arora R, Engle SK, Scott LR and Olgin JE: Tissue structure and connexin expression of canine pulmonary veins. *Cardiovasc Res* 55: 727-738, 2002.
18. Arora R, Verheule S, Scott L, Navarrete A, Katari V, Wilson E, Vaz D and Olgin JE: Arrhythmogenic substrate of the pulmonary veins assessed by high-resolution optical mapping. *Circulation* 107: 1816-1821, 2003.
19. Hollands C: The Animals (scientific procedures) Act 1986. *Lancet* 2: 32-33, 1986.
20. Combes RD and Balls M: The Three Rs-opportunities for improving animal welfare and the quality of scientific research. *Altern Lab Anim* 42: 245-259, 2014.
21. Chandler NJ, Greener ID, Tellez JO, Inada S, Musa H, Molenaar P, Difrancesco D, Baruscotti M, Longhi R, Anderson RH, *et al*: Molecular architecture of the human sinus node: Insights into the function of the cardiac pacemaker. *Circulation* 119: 1562-1575, 2009.
22. Mueller-Hoecker J, Beitingner F, Fernandez B, Bahlmann O, Assmann G, Troidl C, Dimomeletis I, Käb S and Deindl E: Of rodents and humans: A light microscopic and ultrastructural study on cardiomyocytes in pulmonary veins. *Int J Med Sci* 5: 152-158, 2008.
23. Logantha SJ, Cruickshank SF, Rowan EG and Drummond RM: Spontaneous and electrically evoked Ca²⁺ transients in cardiomyocytes of the rat pulmonary vein. *Cell Calcium* 48: 150-160, 2010.
24. Spach MS, Barr RC and Jewett PH: Spread of excitation from the atrium into thoracic veins in human beings and dogs. *Am J Cardiol* 30: 844-854, 1972.
25. Ehrlich JR, Cha TJ, Zhang L, Chartier D, Melnyk P, Hohnloser SH and Nattel S: Cellular electrophysiology of canine pulmonary vein cardiomyocytes: Action potential and ionic current properties. *J Physiol* 551: 801-813, 2003.
26. Boyett MR, Honjo H and Kodama I: The sinoatrial node, a heterogeneous pacemaker structure. *Cardiovasc Res* 47: 658-687, 2000.
27. Boyett MR, Inada S, Yoo S, Li J, Liu J, Tellez J, Greener ID, Honjo H, Billeter R, Lei M, *et al*: Connexins in the sinoatrial and atrioventricular nodes. *Adv Cardiol* 42: 175-197, 2006.
28. Dobrzynski H, Boyett MR and Anderson RH: New insights into pacemaker activity: Promoting understanding of sick sinus syndrome. *Circulation* 115: 1921-1932, 2007.
29. Saez JC, Berthoud VM, Branes MC, Martinez AD and Beyer EC: Plasma membrane channels formed by connexins: Their regulation and functions. *Physiol Rev* 83: 1359-1400, 2003.
30. Severs NJ, Bruce AF, Dupont E and Rothley S: Remodelling of gap junctions and connexin expression in diseased myocardium. *Cardiovasc Res* 80: 9-19, 2008.
31. Bikou O, Thomas D, Trappe K, Lugenbiel P, Kelemen K, Koch M, Soucek R, Voss F, Becker R, Katus HA and Bauer A: Connexin 43 gene therapy prevents persistent atrial fibrillation in a porcine model. *Cardiovasc Res* 92: 218-225, 2011.
32. Igarashi T, Finet JE, Takeuchi A, Fujino Y, Strom M, Greener ID, Rosenbaum DS and Donahue JK: Connexin gene transfer preserves conduction velocity and prevents atrial fibrillation. *Circulation* 125: 216-225, 2012.
33. Yamamoto M, Dobrzynski H, Tellez J, Niwa R, Billeter R, Honjo H, Kodama I and Boyett MR: Extended atrial conduction system characterised by the expression of the HCN4 channel and connexin45. *Cardiovasc Res* 72: 271-281, 2006.
34. Perez-Lugones A, McMahon JT, Ratliff NB, Saliba WI, Schweikert RA, Marrouche NF, Saad EB, Navia JL, McCarthy PM, Tchou P, *et al*: Evidence of specialized conduction cells in human pulmonary veins of patients with atrial fibrillation. *J Cardiovasc Electrophysiol* 14: 803-809, 2003.
35. Morel E, Meyronet D, Thivoleat-Bejuy F and Chevalier P: Identification and distribution of interstitial Cajal cells in human pulmonary veins. *Heart Rhythm* 5: 1063-1067, 2008.
36. Li YD, Hong YF, Zhang Y, Zhou XH, Ji YT, Li HL, Hu GJ, Li JX, Sun L, Zhang JH, *et al*: Association between reversal in the expression of hyperpolarization-activated cyclic nucleotide-gated (HCN) channel and age-related atrial fibrillation. *Med Sci Monit* 20: 2292-2297, 2014.
37. Priori SG, Pandit SV, Rivolta I, Berenfeld O, Ronchetti E, Dhamoon A, Napolitano C, Anumonwo J, di Barletta MR, Gudappakkam S, *et al*: A novel form of short QT syndrome (SQT3) is caused by a mutation in the KCNJ2 gene. *Circ Res* 96: 800-807, 2005.
38. Chen YJ, Chen SA, Chen YC, Yeh HI, Chan P, Chang MS and Lin CI: Effects of rapid atrial pacing on the arrhythmogenic activity of single cardiomyocytes from pulmonary veins: Implication in initiation of atrial fibrillation. *Circulation* 104: 2849-2854, 2001.
39. Melnyk P, Ehrlich JR, Pourrier M, Villeneuve L, Cha TJ and Nattel S: Comparison of ion channel distribution and expression in cardiomyocytes of canine pulmonary veins versus left atrium. *Cardiovasc Res* 65: 104-116, 2005.
40. Marks AR: Calcium cycling proteins and heart failure: Mechanisms and therapeutics. *J Clin Invest* 123: 46-52, 2013.
41. Frank KF, Böck B, Erdmann E and Schwinger RH: Sarcoplasmic reticulum Ca²⁺-ATPase modulates cardiac contraction and relaxation. *Cardiovasc Res* 57: 20-27, 2003.
42. Musa H, Lei M, Honjo H, Jones SA, Dobrzynski H, Lancaster MK, Takagishi Y, Henderson Z, Kodama I and Boyett MR: Heterogeneous expression of Ca(2+) handling proteins in rabbit sinoatrial node. *J Histochem Cytochem* 50: 311-324, 2002.
43. Lyashkov AE, Juhaszova M, Dobrzynski H, Vinogradova TM, Maltsev VA, Juhasz O, Spurgeon HA, Sollott SJ and Lakatta EG: Calcium cycling protein density and functional importance to automaticity of isolated sinoatrial nodal cells are independent of cell size. *Circ Res* 100: 1723-1731, 2007.
44. Thiagalingam A, Reddy VY, Cury RC, Abbara S, Holmvang G, Thangaraoopam M, Ruskin JN and d'Avila A: Pulmonary vein contraction: Characterization of dynamic changes in pulmonary vein morphology using multiphase multislice computed tomography scanning. *Heart Rhythm* 5: 1645-1650, 2008.
45. Rietdorf K, Masoud S, McDonald F, Sanderson MJ and Bootman MD: Pulmonary vein sleeve cell excitation-contraction-coupling becomes dysynchronized by spontaneous calcium transients. *Biochem Soc Trans* 43: 410-416, 2015.
46. Bogdanov KY, Vinogradova TM and Lakatta EG: Sinoatrial nodal cell ryanodine receptor and Na(+)-Ca(2+) exchanger: Molecular partners in pacemaker regulation. *Circ Res* 88: 1254-1258, 2001.
47. Honjo H, Boyett MR, Niwa R, Inada S, Yamamoto M, Mitsui K, Horiuchi T, Shibata N, Kamiya K and Kodama I: Pacing-induced spontaneous activity in myocardial sleeves of pulmonary veins after treatment with ryanodine. *Circulation* 107: 1937-1943, 2003.